

# Monzonorites from Rogaland (Southwest Norway): a Series of Rocks Coeval but not Comagmatic with Massif-type Anorthosites

J.C. DUCHESNE<sup>1</sup>, E. WILMART<sup>1,2</sup>, D. DEMAIFFE<sup>3</sup> and J. HERTOGEN<sup>4</sup>

<sup>1</sup>Lab. ass. Géologie, Pétrologie et Géochimie, Université de Liège, B 4000 Sart Tilman (Belgium)

<sup>2</sup>Laboratoire Pierre Süe, Groupe des Sciences de la Terre, CEN Saclay, F 91191 Gif-sur-Yvette (France)

<sup>3</sup>Lab. ass. Géologie, Pétrologie et Géochronologie, Université Libre de Bruxelles, B 1050 Bruxelles (Belgium)

<sup>4</sup>Afdeling Fysico-Chemische Geologie, Katholieke Universiteit Leuven, B 3000 Leuven (Belgium)

(Received March 20, 1988; revision accepted March 10, 1989)

## Abstract

Duchesne, J.C., Wilmart, E., Demaiffe, D. and Hertogen, J., 1989. Monzonorites from Rogaland (Southwest Norway): a series of rocks coeval but not comagmatic with massif-type anorthosites. *Precambrian Res.*, 45: 111–128.

Monzonorites, members of the anorthositic suite of rocks, are usually considered as residual after the formation of massif-type anorthosites. In Rogaland (S.W. Norway) they occur as large dykes, intrusions and chilled margins to differentiated massifs, emplaced during and soon after the main anorthosite massifs, in granulite facies conditions.

Ti, P and Fe are enriched in monzonorites and steadily decrease towards quartz mangerites, the FeO/FeO + MgO ratios varying slightly during alkali enrichment (Bowen trend). Trace element spidergrams show deep troughs in Rb, Th, Nb-Ta, Sr, Zr-Hf and Ti. The REE slightly decrease in the evolution with (La/Yb)<sub>N</sub> ratios about 9 and neutral to positive Eu anomalies. Several occurrences, however, show highly contrasted trace element features.

Sr isotope ratios ( $I_{Sr}$ ) show a wide interval of variation (0.704–0.710) between the various dykes and intrusions without any correlation with the elements indicative of crustal contamination. In the Tellnes main dyke, evolution towards acidic rocks occurs without contamination and variation in  $I_{Sr}$ . Fractional crystallization with subtraction of apatite-bearing noritic cumulates can account for the major and trace element evolution from monzonorite to quartz mangerite, but is unable to explain the large differences between occurrences.

It is concluded that monzonorites cannot be comagmatic (though coeval) with massif-type anorthosites. They result from the crystallization of distinct magma batches, possibly formed through partial melting of basic to intermediate rocks in the lower crust.

## Introduction

Monzonorites (=hypersthene monzodiorites=jotunites) constitute an important member of the Proterozoic anorthosite suite of rocks. They occupy a key position between the anorthosite-norite group and the K-rich rocks (mangerite=hypersthene monzonite, quartz mangerite=hypersthene quartz monzonite and charnockite=hypersthene granite), though

volumetrically of a lesser importance than the other rocks.

They are classically considered as residual liquids left over by the fractional crystallization of the massif-type anorthosites (Buddington, 1972; Morse, 1982; Ashwal, 1982). They indeed have chemical characters (high Fe, Ti and P contents) which resemble those of ferro-diorites occurring in the upper part of the Skaergaard layered intrusion. Different interpreta-

tions have, however, also been provided. Emslie (1978) has suggested a derivation from a tholeiitic magma through separation of mafic minerals in a subcrustal magma chamber before intrusion in the anorthosite massifs. Duchesne and Demaiffe (1978) have expressed the view that monzonorites were parental to andesine anorthosites. Philpotts (1981) has considered that immiscibility can give rise to conjugated quartz mangeritic liquids and monzonoritic liquids.

Another debated question is the relationship between monzonorites and K-rich rocks. Are the two groups comagmatic, as proposed by Michot (1965) and Philpotts (1966, 1981), or are they simply coeval (Emslie, 1978; Morse, 1982)? What is the exact role of contamination (and/or hybridization) in the development of the kindred? It must be recalled that the geodynamic setting of the Proterozoic massive anorthosites is still open to discussion (Duchesne, 1984; Emslie, 1985). The anorthosite parent magma is difficult to reconstruct because of the simplicity of the mineralogy of the anorthosite itself. Any model thus strongly relies on the significance of the associated intermediate and acidic rocks and prompts a better understanding of their relationship with anorthosite.

The purpose of the present study is to provide new data and to synthesize the available evidence on monzonorites from the Rogaland anorthosite province (S. Norway). It amplifies earlier results on the Hydra massif (Duchesne et al., 1974; Demaiffe and Hertogen, 1981), on the Eia-Rekefjord intrusion (Wiebe, 1984), and on dykes in the Egersund-Ogna massive anorthosite (Duchesne et al., 1985).

It will be shown that (1) there is no direct relationship between massif-type anorthosites and monzonorites; (2) fractional crystallization without contamination (or hybridization) can explain the transition between monzonorites and acidic rocks; and (3) there is no unique parental magma to account for the diversity inside the monzonorite group and several lower crustal sources are required.

## Field relationships and petrographic characters

In the Rogaland anorthosite province, monzonorites occur as dykes and small intrusions. They have also given rise to differentiated bodies of medium to large dimensions. Numerous dykes cut across the three large massif-type anorthosites and the lower part of the Bjerkreim-Sokndal layered body (BKSK) (Fig. 1). They vary in thickness from a few decimetres to several tens of meters and extend up to 20 km in length. Each major dyke has distinctive characters.

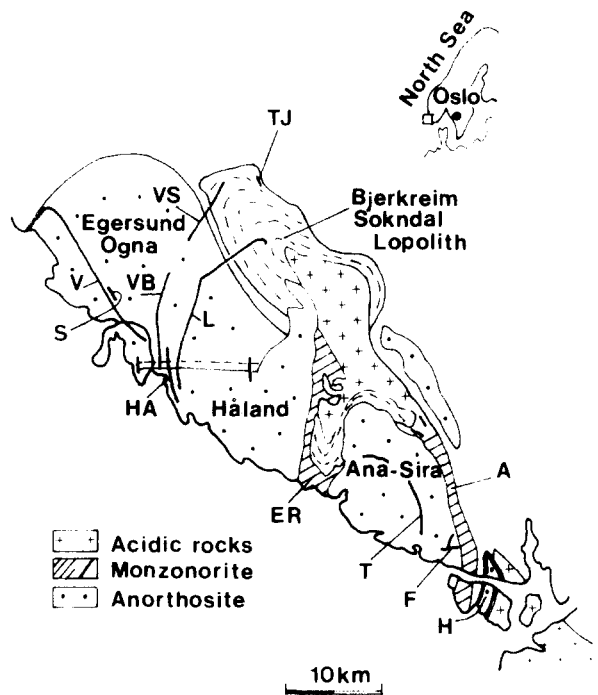


Fig. 1. Schematic geological map of the Rogaland anorthositic complex showing the large massif-type anorthosites, the Bjerkreim-Sokndal lopolith and the most important monzonoritic occurrences. Labels (in alphabetical order): A, Apophysis; ER, Eia-Rekefjord intrusion; F, Fidsel dyke; H, Hydra massif; HA, Håland dyke; L, Lomland dyke; S, Sirevåg dyke; T, Tellnes main dyke; TJ, Tjörn chilled margin; V, Vettaland dyke; VB, Varberg dyke; VS, Vaersland dyke. The Tellnes satellite dykes (SAT) are not distinguished from the Tellnes dyke.

In the Egersund–Ogna massif, the Lomland (L) dyke varies from an antiperthite norite to a monzonorite, the Vettaland (V) dyke is a monotonous granular (quartz) ferronorite, the Varberg (VB) dyke is a monzonorite and the Vaersland (VS) dyke a quartz monzonite (Duchesne et al., 1985), the small monzonoritic Sirevåg (S) dyke is also worth mentioning. In the Åna–Sira massif, the Tellnes (T) main dyke, gradually changes from monzonorite to quartz mangerite. Closely associated with the latter, fine-grained monzonorites occur in Tellnes satellite (SAT) dykes (Wilmart et al., 1989). In the Håland massif, the Håland (HA) dyke also shows a conspicuous variation from norite to charnockite.

The small intrusion of Hydra (H) (Duchesne et al., 1974; Demaiffe and Hertogen, 1981) displays a monzonoritic inner margin and a central part made up of anorthosite and leuconorite, and is cut across by a stockwork of charnockitic dykes. The Eia–Rekefjord (ER) intrusion (Michot, 1960; Wiebe, 1984) was intruded later than the neighbouring anorthosites of Håland–Helleren and the norites of the southern lobe of BKSK into which it sends monzonoritic dykes. It is, however, more or less contemporaneous with the upper part of BKSK, as suggested by the occurrence of pillow-like inclusions in the quartz mangerites (Wiebe, 1984). A similar relationship is also found in the apophysis (A), east of the Åna–Sira massif: fine-grained pillow-like monzonorites (A1) commingled with coarser-grained mangeritic material (A2). A fine-grained monzonorite has also been found at Tjörn (TJ), at the contact of BKSK and its envelope. Duchesne and Hertogen (1988) have emphasized that this rock could represent the parental magma of the series of cumulates which constitutes the lower part of the lopolith and ranges from anorthosite at the base to norites and finally mangerites on top (Michot, 1965; Duchesne et al., 1987).

Monzonoritic magmatism has spanned over a long period of time in the igneous history of the province. It has started with the intrusion

of BKSK, continued with the dyke system, then with the commingling of K-rich rocks. A minor dyking episode (Fidsel dyke) (F) occurred at the end of the apophysis development. The Hydra massif, clearly post-tectonic, also closed the evolution. Absolute ages in the interval of 950–930 Ma have been obtained for Tellnes (Wilmart et al., 1989) and Hydra (Pasteels et al., 1979).

Petrographically, the rock texture varies from subophitic norites to slightly porphyritic mangerites. Equigranular monzonorites are very common. Fine-grained “chilled” varieties occur locally at the contact of the large dykes, in some thin dykelets or in rounded pillow-like inclusions when commingled with K-rich material. The chilled rocks plot on the same trends as the coarser-grained rocks in the variation diagram B, thus suggesting that, whatever the texture, most rocks were emplaced as magmatic liquids unladen with already crystallized minerals.

Unzoned antiperthitic plagioclase (andesine), inverted pigeonite, hemo-ilmenite, magnetite and apatite characterize the norites. With increasing acidity, the mafics content decreases, while the plagioclase is progressively replaced by a mesoperthitic feldspar and the opx content decreases relatively to cpx. A typical variation in the Fe number is displayed in the Tellnes dyke where the opx passes from  $En_{36}$  in the monzonorite to  $En_{17}$  in the quartz mangerites. Crystallization has taken place under granulite facies conditions. Thermobarometric and fluid inclusion studies in the Tellnes dyke and in the upper part of BKSK (Wilmart and Duchesne, 1987; Wilmart, 1988) yield pressure of about  $7.5 \pm 1$  kbar,  $\log f_{O_2} = -15 \pm 0.5$  atm at  $\sim 800^\circ\text{C}$ , that is lower than the FMQ buffer and close to the  $\text{CO}_2 \rightleftharpoons \text{C} + \text{O}_2$  reaction, and show that a pure  $\text{CO}_2$ -fluid was present when the (acidic) rocks crystallized.

### Geochemical characters

A total of 130 samples from 14 different geological units have been analysed for major and

trace elements. Representative analyses are given in Table I.

### Major elements

The rocks form a continuous succession with respect to  $\text{SiO}_2$  concentrations (42–67%). The most basic members are characterized by relatively high Fe, Ti and P contents which steadily decrease with increasing acidity (Fig. 2b). The suite of rocks starts at the limit of silica saturation and ends with normative quartz content, which does not exceed 25% of the leucocratic minerals.  $\text{K}_2\text{O}$  varies from 0.5 to 5.5% (Fig. 2a),  $\text{Al}_2\text{O}_3$  remains low, and the algaïtic index reaches 0.8 in the most acidic members only. The alkali–lime index indicates alkali–calcic characters, except for the Vettaland ferronorite which show sub-alkaline affinities. The AFM diagram (Fig. 3) indicates a large variation in the F/M ratios between the different geological units, each unit showing a virtually constant ratio (Bowen trend). Three major groups can be distinguished: the Vettaland dyke has a ratio of  $\sim 0.90$  and a very restricted evolution towards alkali enrichment. A second group with a ratio of 0.76 comprises the Hidra and Tjörn chilled margins as well as the pillows from the apophysis. The other occurrences have ratios between 0.80 and 0.85. Small but significant variations in the major element contents can also be observed between the different occurrences as illustrated by Fig. 2.

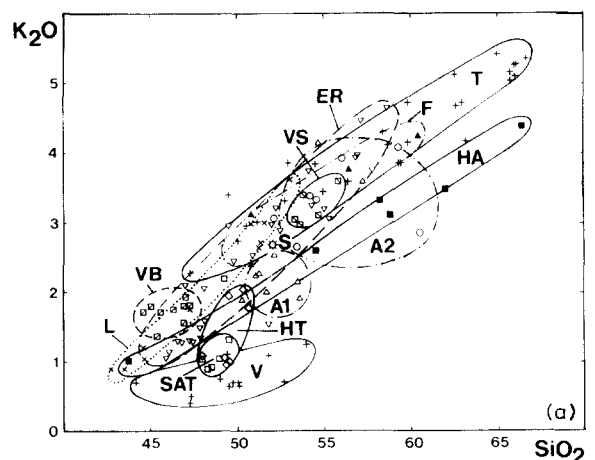
### Trace elements

The most important variation in trace element content is found in the Tellnes dyke (Figs. 2b and 4), which can therefore be used to describe the element distribution and evolution in the population, except for some cases that will be discussed later. In spidergrams, monzonorites show a plateau for most elements at normalized values between 100 and 200, a smooth decrease down to 20 to the right of the diagram, and deep troughs for Rb, Th, Nb–Ta, Sr, Zr–Hf

and Ti. In the evolution towards acidic rocks, most elements, including the REE (Fig. 5), decrease except K, Ba, Rb, Zr and Hf. The Eu anomaly is slightly positive (Fig. 5; Table I) in monzonorites and becomes more positive with increasing acidity. When passing from basic to acidic rocks (Table I),  $(\text{La}/\text{Yb})_N$  slightly decreases from about 12 down to 5, K/Rb ratios vary from 1200 down to 600 and K/Ba from 15 to 30. Zr/Hf ratios remain around 40. U and Th are very low (usually less than 0.5 ppm and 0.8 ppm, respectively) and vary erratically. Ni and Cr are very low (less than 20 ppm). In the evolution towards acidic rocks, Sc decreases by a factor 2 (30–15 ppm), Co by a factor 4 (40–10 ppm), Zn decreases slightly from 200 ppm to 150 ppm and V varies erratically between 20 and 130 ppm.

Similar contents and behaviour with slight variants are also observed in the Lomland, Vaersland, Varberg and Håland dykes and in the apophysis. Variation diagrams (Fig. 2), however, show that each occurrence has its own fingerprints (variable contents, extent of evolution, values of the slope in variation diagrams). Also note the enrichment in U and Th in the apophysis and the variation in the Zr/Hf ratios from 25 to 47 between the two facies of the Lomland dyke.

However, some occurrences depart signifi-



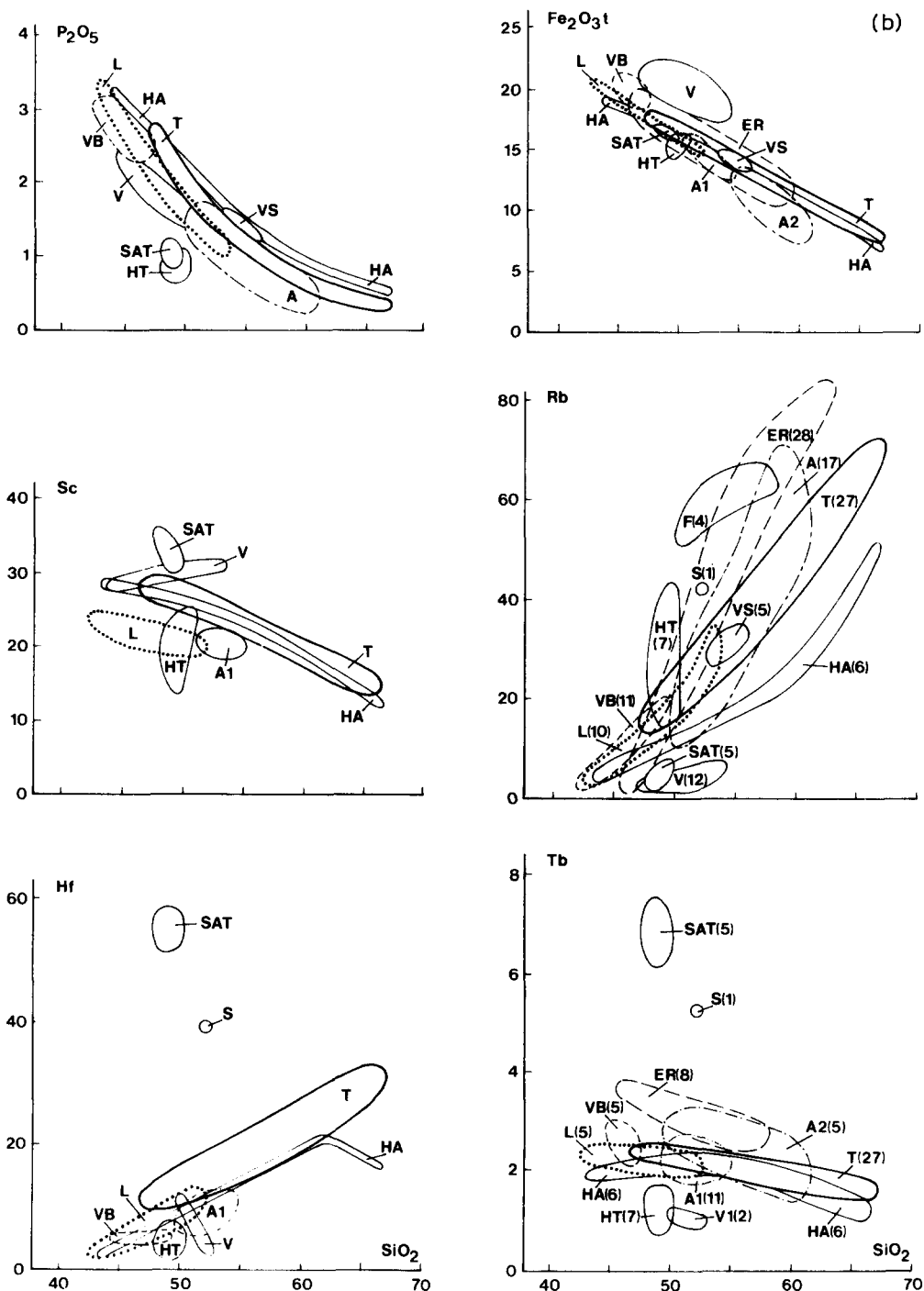


Fig. 2. Variation diagrams for representative major (%) and trace (ppm) element evolution. The various clusters enclose the data from the various occurrences (list of abbreviations in the text and in Fig. 1). The rocks from Tjörn and Hidra chilled margins have been grouped under label HT. In (a) the position of the various rocks are represented inside each cluster. In (b) only the clusters are represented. For  $K_2O$ ,  $P_2O_5$ ,  $Fe_2O_3$  and Rb, the number of samples analysed in each occurrence is indicated in the Rb diagram by the figure in parentheses following the label. For Sc, Hf and Tb, the number of samples is indicated in a similar way in the Tb diagram.

TABLE 1

Representative analyses of monzonorites<sup>a</sup>

	Tellnes				Håland				Lomland				
	7252	7828	7832	QMANG	81323	7548	66201	72136	66175	7353	72105	PUNT	KLUN
SiO <sub>2</sub>	47.32	56.38	65.71	65.87	43.76	58.78	61.97	66.43	42.75	47.29	51.35	43.88	51.60
TiO <sub>2</sub>	3.00	1.00	0.99	1.08	4.00	2.19	1.87	1.34	4.36	3.56	2.40	4.44	2.41
Al <sub>2</sub> O <sub>3</sub>	12.80	14.00	13.31	13.41	13.48	13.52	13.50	13.36	12.18	13.34	15.01	12.89	14.65
Fe <sub>2</sub> O <sub>3</sub>	4.53	4.42	2.72	2.82	5.79	3.43	2.39	1.64	6.83	4.08	3.81	5.13	4.90
FeO	11.96	7.87	5.09	5.10	11.96	7.41	7.27	5.05	12.43	12.62	10.15	13.20	8.87
MnO	0.21	0.16	0.11	0.13	0.25	0.17	0.14	0.11	0.26	0.27	0.21	0.26	0.19
MgO	3.44	1.69	0.65	0.63	4.09	1.97	1.00	1.26	4.26	3.58	2.22	3.94	2.26
CaO	7.43	4.66	2.56	2.18	8.72	4.88	4.00	3.14	9.13	7.65	6.31	8.76	6.21
Na <sub>2</sub> O	3.53	3.31	3.07	3.20	3.44	3.72	3.29	3.11	3.01	3.59	3.94	3.26	3.96
K <sub>2</sub> O	2.28	3.00	5.04	5.23	1.02	3.11	3.49	4.39	0.90	1.76	2.72	1.02	3.00
P <sub>2</sub> O <sub>5</sub>	2.74	1.04	0.51	0.42	3.26	1.11	0.98	0.60	3.40	2.18	1.49	2.99	1.44
Tot	99.82	99.03	99.76	100.08	100.17	100.29	100.80	100.43	99.51	99.92	99.61	99.76	99.49
U	0.32	0.18	0.20	0.19	0.20	0.24	0.18	0.53	0.31		0.16	0.30	0.22
Th	0.79	0.59	0.66	0.55	0.59	0.31	0.52	1.79	0.71		0.30	0.60	0.39
Zr	442	717	1387	1254	84	770	1146	772	56	89	369	70	482
Hf	11.00	17.30	32.50	31.19	2.00	17.4	21.30	16.90	2.57		8.27	2.78	10.20
Ta	1.68	1.27	0.94	1.01	1.28	1.21	1.11	1.27	1.05		1.18	0.58	0.82
Th/U	2.5	3.3	3.3	2.9	3.0	1.3	2.9	3.4	2.3		1.9	2.0	1.8
Zr/Hf	40	41	43	40	42	44	54	46	22		45	25	47
Rb	16.3	32.6	68.8	68.9	4.0	23.5	30.3	50.6	5.1	9.7	16.9	5.3	21.9
Sr	366	294	142	152	556	335	399	308	438	417	447	458	393
Ba	1212	1553	1482	1464	674	1747	1746	1933	576	1451	1857	721	1799
K/Rb	1161	764	608	630	2117	1098	956	720	1465	1506	1336	1582	1138
K/Ba	16	16	28	30	13	15	17	19	13	10	12	12	14
Sc	26.3	21.1	16.0	15.4	28.9	18.4	17.2	12.6	24.8		21.2	11.3	12.3
V	128	35	72	44	218	75	67	35	171	110	70	160	73
Cr <sup>b</sup>	1.5					2.3			2.7		1.0	1.1	0.7
Co	36	18	7	7	46	21	17	12	51	38	27	46	22
Ni <sup>b</sup>													
Zn	197	186	151	147	196	155	138	101	200	221	182	202	186
La	54.7	47.5	33.7	37.0	40.2	47.2	41.5	36.1	42.4	37.0	37.8	41.0	42.1
Ce	138	113	77	83	92	110	95	75	109	98	92	104	103
Nd	106.0	83.0	57.0	56.7	63.0	67.6	69.0	41.0	72.7	68.0	60.4	71.0	64.9
Sm	20.4	16.2	11.7	11.9	13.4	15.9	10.2	8.0	20.1		15.6	19.0	16.5
Eu	7.00	6.00	5.00	5.77	6.00	5.69	4.00	4.00	6.82		7.69	6.80	7.53
Tb	2.00	2.11	1.68	1.74	1.98	1.88	1.52	1.17	2.39		1.90	2.27	2.08
Yb	3.00	3.00	4.00	4.57	2.00	3.51	3.00	2.00	2.78		2.75	2.63	3.01
Lu	0.42	0.53	0.61	0.77		0.54			0.43		0.39	0.39	0.45
Y	79	78	52	61	76	44	58	38	53	51	46	51	52
(La/Yb) <sub>N</sub>	12.1	10.5	5.6	5.4	13.4	8.9	9.2	12.0	10.1		9.1	10.3	9.3
Eu/Eu*	1.1	1.2	1.3	1.5	1.4	1.0	1.2	1.5	1.1		1.6	1.1	1.4

<sup>a</sup>Major elements (%), trace elements (ppm).<sup>b</sup>Unless specified, less than 20 ppm.

Vaersland		Varberg		Apophysis					Vettaland			
66192	VAER	7520AV	VARB	811281	811282	PIL	ALG	FID	7529	HET	7557	EIGER
55.82	54.26	45.96	46.45	51.71	52.10	52.83	56.11	54.60	44.19	49.68	52.68	49.55
2.24	2.43	3.77	3.70	3.53	2.39	3.05	1.70	2.16	3.02	2.60	2.41	3.01
13.39	13.74	12.64	12.83	13.72	15.48	14.28	16.23	14.04	14.13	12.78	13.01	13.27
3.27	5.55	4.46	4.63	2.85	5.97	2.83	4.23	5.44	4.61	7.48	3.77	4.32
9.70	7.92	13.10	13.11	11.12	8.08	10.00	6.41	7.82	15.86	12.22	13.61	13.98
0.19	0.20	0.21	0.23	0.20	0.21	0.17	0.15	0.21	0.26	0.27	0.25	0.24
1.96	2.24	3.35	3.41	3.72	1.41	3.71	1.51	1.87	2.35	2.09	2.22	2.84
5.20	5.48	8.25	7.84	6.38	5.85	5.78	4.96	5.05	9.10	7.38	7.05	7.79
3.24	3.34	3.25	3.46	4.21	4.69	4.16	4.81	3.83	2.89	2.78	2.95	2.96
3.60	3.23	1.76	1.77	2.01	3.07	2.53	3.45	3.38	0.70	0.98	0.72	0.62
1.30	1.51	2.69	2.56	1.00	0.91	1.03	0.63	1.07	2.41	1.67	1.37	1.52
99.91	99.90	99.44	100.05	100.65	100.16	100.51	100.17	99.65	99.53	100.07	100.05	100.12
0.20		0.30	0.30	1.00	0.28	0.62	0.57	0.20	0.26		0.11	
0.20		0.57	0.71	3.06	1.00	1.84	2.91	0.69	0.30		0.2	
867	727	204	305	347	353	446	655	987	289	1021	70	89
18.10		5.17	5.23	9.00	11.30	11.04	17.72	23.53	6.05		2.80	
1.54		1.79	1.80	1.33	1.15	1.28	0.83	1.59	1.37		0.10	
1.0		1.2	2.4	3.1	3.6	3.0	5.1	3.5	1.2		2	
48		39	58	39	31	40	37	42	48		25	
34.4	34.4	11.0	11.9	23.0	36.0	28.9	44.3	29.6	3.9	5.4	4.3	2.3
294	338	400	406	361	392	373	373	328	607	537	571	570
1403	1561	1253	1181	754	1648	910	1388	1902	491	713	593	452
869	780	1328	1233	726	708	725	647	949	1490	1524	1390	2221
21	17	12	12	22	15	23	21	15	12	11	10	11
18.8		27.8	27.9	20.0	23.9	17.3	18.3	20.5	28.3		30.9	30.7
58	58	162	156	175	73	141	46	58	84	40	50	115
1.1		2.9	2.9	7.0	8.0	4.5	3.9	2.0	1.3		1.4	1.8
21		38	34	41	24	38	17	21	33	28	33	35
		22	22	25		18						15
158		216	215	154	188	135	136	231	268	235	215	206
44.8		55.8	57.8	42.1	54.1	36.0	45.0	54.2	51.0	44.5	6.3	7.3
112	110	135	140	104	134	101	104	130	130	128	18	30
66.2		88.0	91.0	65.0	94.0	54.8	68.7	83.7	90.2	72.4	19.0	23.0
17.2		18.8	18.3	14.0	20.6	12.1	15.3	18.7	25.7		7.1	7.6
6.49		7.90	7.78	4.37	7.04	4.04	6.20	7.19	7.97		4.93	5.00
2.15		2.63	2.62	2.09	3.25	1.79	2.39	2.45	3.54		0.94	1.05
3.71		4.18	4.33	5.00	7.00	4.19	5.82	4.00	4.51		1.72	1.82
0.57		0.74	0.74	0.75	1.15	0.65	0.90	0.74	0.65		0.25	0.29
53	56	80	74	63	96	62	73	76	86	84	26	33
8.0		8.9	8.9	5.6	5.1	5.7	5.1	9.0	7.5		2.4	2.7
1.2		1.3	1.3	1.0	1.0	1.0	1.2	1.2	1.0		2.2	2.0

TABLE 1 (continued)

	Sat		Sirevåg	Hidra-Tjörn			
	842	SAT	75542	7234	7020	80123	HITJ
SiO <sub>2</sub>	48.32	48.68	52.02	49.53	48.00	49.39	49.54
TiO <sub>2</sub>	2.54	2.41	2.14	3.82	4.61	3.67	4.17
Al <sub>2</sub> O <sub>3</sub>	16.62	16.14	15.04	14.50	14.20	15.81	14.06
Fe <sub>2</sub> O <sub>3</sub>	6.45	7.09	4.38	2.00	5.00	5.81	5.11
FeO	9.37	8.67	9.64	11.70	10.40	7.88	9.50
MnO	0.28	0.23	0.23	0.17	0.18	0.13	0.16
MgO	2.00	2.55	2.14	4.00	4.00	4.54	4.87
CaO	7.87	8.12	6.21	6.00	6.00	6.87	6.56
Na <sub>2</sub> O	4.14	4.11	4.05	3.00	3.00	3.00	3.50
K <sub>2</sub> O	0.90	1.04	2.69	1.95	1.08	0.96	1.41
P <sub>2</sub> O <sub>5</sub>	1.15	1.03	1.01	0.91	0.81	0.71	1.03
Tot	100.14	100.09	99.55	99.83	99.81	99.17	99.91
U	0.76	0.57	0.53	1.19	0.85	0.10	1.13
Th	2.69	3.31	2.11	3.00	1.96	0.50	2.75
Zr	1863	2229	1591	300	174	262	191
Hf	57.30	55.56	39.40	7.00	5.00	6.00	5.27
Ta	0.92	1.16	1.88	1.22	1.02	1.31	1.09
Th/U	3.5	5.8	4.0	2.5	2.3	5.0	2.4
Zr/Hf	33	40	40	43	35	44	36
Rb	2.0	4.5	42	43.0	19.4	17.0	23.9
Sr	593	521	347	382	450	530	435
Ba	562	581	1613	580	450	469	576
K/Rb	3736	1910	532	376	462	469	490
K/Ba	13	15	14	28	20	17	20
Sc	34.3	33.4	27.6	20.0	20.8	13.8	20.5
V	157	94	66	300	250		222
Cr <sup>b</sup>			9	32	38	28	17
Co	27	22	21	47	48	49	47
Ni <sup>b</sup>	52	23		55	20	60	34
Zn	280	276	221				136
La	164.2	165.6	102.0	35.3	30.3	23.9	31.6
Ce	412	430	254	82	75	58	76
Nd	296.0		161.0	52.9	46.6	39.6	48.9
Sm	58.1	53.4	38.1	11.5	11.7	8.0	10.7
Eu	6.00	6.57	7.22	3.31	3.35	2.86	3.33
Tb	7.53	6.89	5.29	1.59	1.58	1.13	1.53
Yb	16.30	18.32	13.10	3.55	3.21	2.00	3.17
Lu	2.26	0.45	2.08	0.52	0.54	0.33	0.51
Y	295	268	144			22	36
(La/Yb) <sub>N</sub>	6.7	6.0	5.2	6.6	6.3	7.9	6.6
Eu/Eu*	0.3	0.4	0.6	0.9	0.9	1.1	1.0

TABLE 1 (continued)

Sample location (NGU coordinates) and description		
7252	Tellnes main dyke	Monzonorite, Tellnes open pit LK478.699
7828	Tellnes main dyke	Mangerite, 500 m NWW from 7252 LK473.700
7832	Tellnes main dyke	Quartz mangerite, Botnevatnet LK523.628
Qmang	Tellnes main dyke	Average of 7 quartz mangerites
81323	Håland dyke	Norite, S. Nödland LL265.772
7548	Håland dyke	Monzonorite, S. Egersund LL261.795
66201	Håland dyke	Quartz mangerite, S. Egersund LL261.796
72136	Håland dyke	Quartz mangerite, S. Egersund LL261.796
66175	Lomland dyke	Norite, Puntavoll LL264.806
7353	Lomland dyke	Monzonorite, E. Smörasen LL276.880
72105	Lomland dyke	Monzonorite, Klungland LL301.903
Punt	Lomland dyke	Puntavoll facies: average of 4 rocks
Klung	Lomland dyke	Klungland facies: average of 5 rocks
66192	Vaersland dyke	Quartz monzonite, road to Klögtveit LL286.977
Vaer	Vaersland dyke	Average of 5 rocks
7520AV	Varberg dyke	Monzonorite, Varbergkaien, Egersund LL245.827
Varb	Varberg dyke	Average of 11 rocks, except for NAA data (5 rocks)
811281	Apophysis	Fine-grained monzonorite (pillow), Trolldalen LK570.623
811282	Apophysis	Porphyric monzonorite (containing 811281), Trolldalen LK570.623
Pil	Apophysis	Average of 9 fine-grained monzonorites
Alg	Apophysis	Average of 6 coarse-grained monzonorites
Fid	Apophysis	Average of 4 rocks of the Fidsel dyke
7529	Vettaland dyke	Ferrodiorite, Heresvela LL148.953
Het	Vettaland dyke	Hetland facies: average of 5 rocks
7557	Vettaland dyke	Ferrodiorite, Holmavatnet LL1497.863
Eiger	Vettaland dyke	Eigerøy facies: average of 6 rocks, except for NAA data (2 rocks)
842	Tellnes satellite dykes	Fine-grained monzonorite, SE. Slottheiknuten LK531.613
Sat	Tellnes satellite dykes	Average of 5 rocks from 2 dykes
75542	Sirevåg dyke	Monzonorite, Little Sirevåg LL205.859
7234	Hidra massif	Fine-grained monzonorite, Itland LK591.604
7020	Hidra massif	Fine-grained monzonorite, S. Vardefjell LK577.612
80123	Bjerkreim-Sokndal massif	Chilled monzonorite, Tjörn LL354.985
Hitj		Average of 7 monzonorites from Tjörn and the margin of the Hidra massif

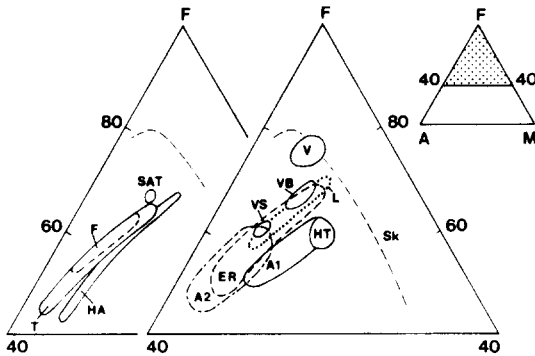


Fig. 3. A  $(\text{Na}_2\text{O}+\text{K}_2\text{O})\text{-F}(\text{FeO}+0.9\text{Fe}_2\text{O}_3)\text{-M}(\text{MgO})$  diagram for the various occurrences (list of abbreviation in the text and in Fig. 1). The broken curve labelled SK represents the Skaergaard liquid evolution.

cantly from this 'normal' distribution. The most striking is the southern part of the Vettaland dyke (Fig. 4), called the Eigerøy facies, which is strongly depleted in most incompatible elements compared with the northern part of the dyke (the Hetland facies) and shows an umbrella-shaped REE distribution with a distinct positive Eu anomaly (Fig. 5) quite distinct from the 'normal' REE distribution in the Hetland facies.

The second case, illustrated in Figs. 4 and 5, comprises the Tellnes satellite dykes (SAT) and the Sirevåg dyke (S). Their REE and Zr-Hf contents are 4–5 times higher than in the Tellnes (T) evolution but the rocks are relatively depleted in Ba, K and Rb. Th is unusually high (up to 5 ppm). A strong negative anomaly ( $\text{Eu}/\text{Eu}^*=0.3\text{--}0.6$ ) characterizes the REE distribution.

The third case comprises the Hidra and Tjörn chilled margins, which show REE distributions similar to the common case but smooth spidergrams with less pronounced troughs for Ta, Sr and Ti. Th remains highly variable (Fig. 4).

#### *Sr isotopes*

Sr isotopic compositions have been determined in whole rocks coming from 9 occur-

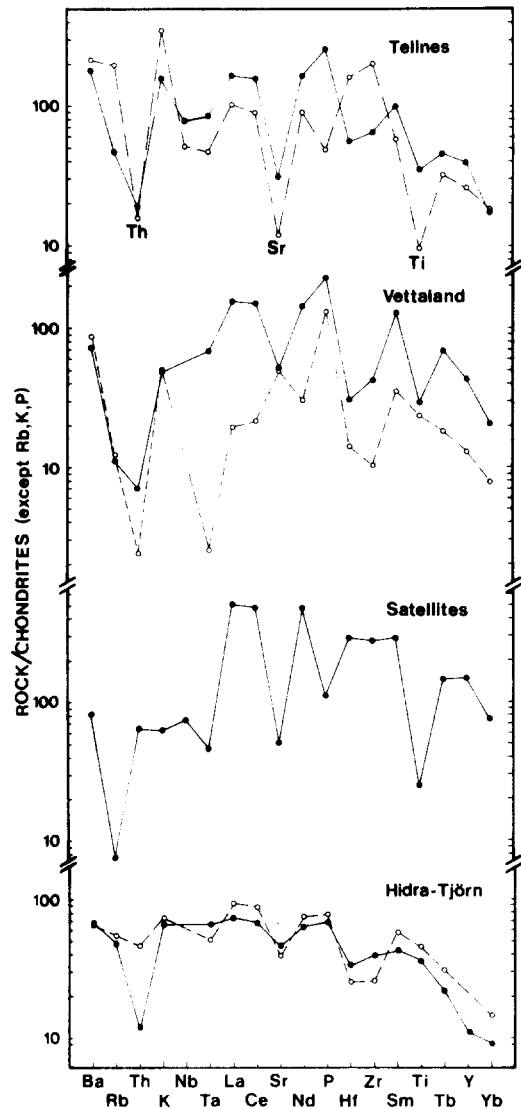


Fig. 4. Chondrite-normalized trace element abundance diagrams (spidergrams) for representative monzonorites and related rocks. The normalization factors are those of Thompson et al. (1983). Tellnes main-dyke evolution (●, monzonorite 7252; ○, quartz mangerite 7832). Vettaland dyke (●, normal facies (Hetland facies) 7529; ○, depleted facies (Eigerøy facies) 7557). Tellnes satellite dykes (monzonorite 842). Hidra and Tjörn chilled margins (●, Tjörn 80123; ○, Hidra 7020).

rences. They are synthesized in Fig. 6. The data for the Vettaland and the Lomland dykes are detailed in Duchesne et al. (1985) and for the

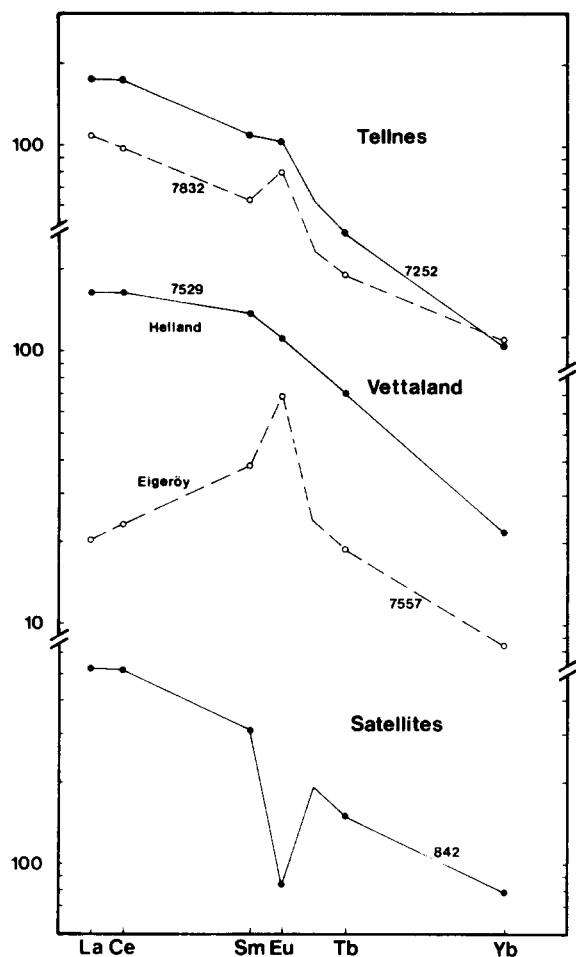


Fig. 5. Chondrite-normalized REE contents of representative monzonorites. Tellnes main dyke (●, monzonorite 7252; ○, quartz mangerite 7832). Vettaland dyke (●, normal facies 7529; ○, depleted facies 7557). Tellnes satellite dykes (monzonorite 842).

Tellnes dyke, in Wilmart et al. (1989). Complementary data are provided here (Table 2) on the Håland dyke, on the Eia-Rekefjord intrusion and on the apophysis, and especially on pillow-like inclusions in coarse-grained mangerite.

The rocks from the Tellnes main dyke plot on an isochron giving an age of  $930 \pm 21$  Ma ( $2\sigma$ ), in close agreement with previous age determinations (Pasteels et al., 1979), and a Sr initial ratio ( $I_{Sr}$ ) of 0.7069. For the Lomland

TABLE 2

Rb-Sr analytical data for the apophysis, the Eia-Rekefjord intrusion and the Håland dyke

	Rb (ppm)	Sr (ppm)	$^{87}\text{Rb}/^{86}\text{Sr}$	$^{87}\text{Sr}/^{86}\text{Sr} \pm 2\sigma$
<i>Apophysis</i>				
7337	56	279	0.583	$0.71502 \pm 0.00010$
C14 mo	56	352	0.463	$0.71306 \pm 0.00008$
C11 Ma	33	328	0.290	$0.71342 \pm 0.00006$
C11 mo	37	378	0.281	$0.70952 \pm 0.00010$
811282	36	392	0.262	$0.71431 \pm 0.00016$
811281	23	361	0.181	$0.70905 \pm 0.00006$
C10 Ma	42	435	0.282	$0.71215 \pm 0.00008$
C10 mo	17.5	336	0.151	$0.70811 \pm 0.00012$
C14 Ma	31	341	0.264	$0.71318 \pm 0.00015$
C13 a	17	367	0.134	$0.70804 \pm 0.00014$
C13 b	29	410	0.202	$0.71102 \pm 0.00014$
C8	20	424	0.137	$0.70837 \pm 0.00007$
7207	24	355	0.198	$0.70898 \pm 0.00020$
<i>Eia-Rekefjord</i>				
78211	26	341	0.219	$0.71057 \pm 0.00018$
7355	13.4	412	0.094	$0.70921 \pm 0.00011$
7354	7.4*	489	0.044	$0.70762 \pm 0.00008$
75672	4.8*	440	0.031	$0.70737 \pm 0.00009$
<i>Håland</i>				
7548	23.5	335	0.203	$0.70965 \pm 0.00004$

Rb and Sr concentrations measured by X-ray fluorescence except those noted by \*, which were measured by isotope dilution.

dyke (Fig. 6B), the pillow-like inclusions of the apophysis and the Eia-Rekefjord intrusion (Fig. 6C), the data points have low  $^{87}\text{Rb}/^{86}\text{Sr}$  ratios (less than 0.22 in Lomland, less than 0.25 for the apophysis) so that they cluster and do not define good isochrons (too large MSWD). They nevertheless plot close to 940 Ma reference isochrons which allow very good estimates of the  $I_{Sr}$ . For the other occurrences (Vettaland dyke, Tellnes orebody, Tellnes satellite dyke), the points plot near the origin so that initial ratios are close to the measured ratios, and  $I_{Sr}$  have been calculated back assuming an age of 940 Ma. The values of  $I_{Sr}$  are reported in Table 3.

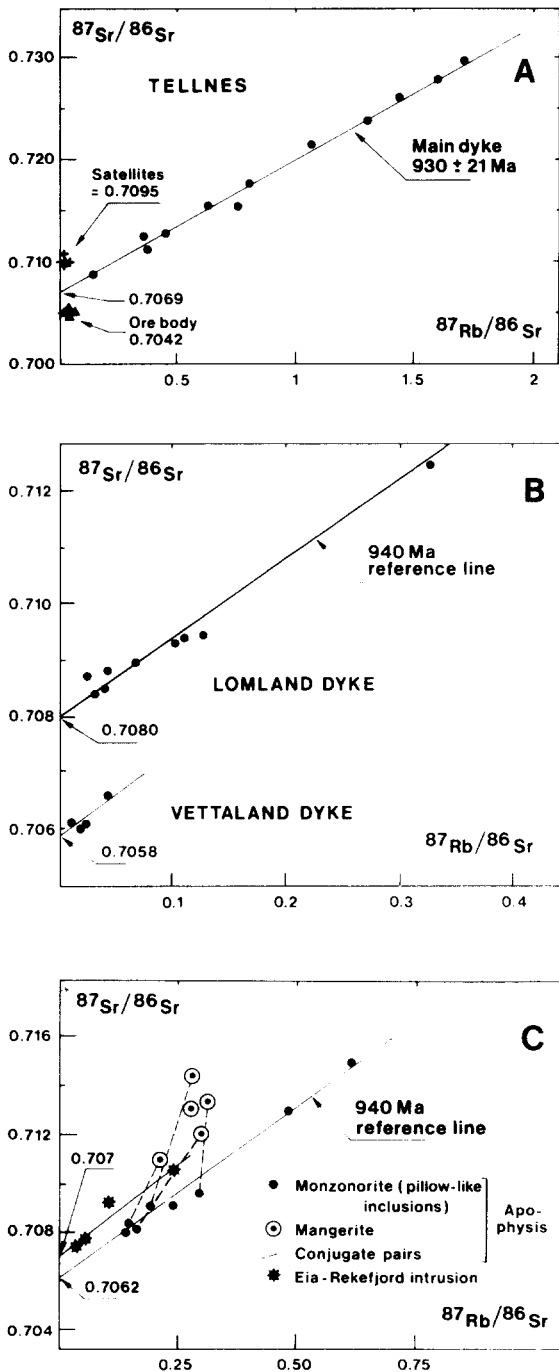


Fig. 6.  $^{87}\text{Sr}/^{86}\text{Sr}$  versus  $^{87}\text{Rb}/^{86}\text{Sr}$  diagrams for various occurrences. A, Tellnes main-dyke, satellite dykes and ore-body. B, Lomland and Vettaland dykes. C, Eia-Rekefjord intrusion and apophysis.

TABLE 3

Strontium isotope initial ratios in monzonorite occurrences

Tjörn	0.7040
Tellnes (orebody)	0.7042
Vettaland	0.7058
Hidra	0.7060
Apophysis (pillows)	0.7062
Håland	0.7067 <sup>a</sup>
Tellnes (main dyke)	0.7069
Eia-Rekefjord	0.7070
Lomland	0.7080
Hidra (acidic dykes)	0.7086
Tellnes (satellites)	0.7100

<sup>a</sup>Recalculated from the data in Table 2 assuming an age of 940 Ma.

## Discussion

### Isotopic constraints

The following pieces of evidence can be drawn from the data:

(1) Large variations in  $I_{\text{Sr}}$  values are observed between the various occurrences. The values fill the gap found in the same area between massif-type anorthosites (0.703–0.706) and K-rich rocks (0.7085) (DemaiFFE et al., 1986).

(2) In two cases (Lomland dyke and Tellnes main dyke), the whole sequence of rocks (which extends from monzonorite to quartz mangerite in Tellnes) plots close to a single isochron which gives the correct age, that is an age corresponding to the U–Pb zircon age. The linear relationships thus cannot be interpreted as mixing lines nor as pseudoisochrons related to contamination of possible mantle melts with crustal components. The relatively small scatter of points around the isochrons is considered to be due to small and erratic degrees of contamination or

to post-magmatic alteration (Rb is well-known to be mobile in granulite facies conditions). If these second-order variations are neglected, the linear relationships imply that all the rocks of each of these dykes are strictly comagmatic and that the differentiation process which linked the monzonorites to more K-rich rocks can have taken place in a closed system without progressive contamination. This is, however, by no means a general rule. In the Hidra body, differentiation from monzonorite to acidic rocks (stockwork) was accompanied by contamination, as put forward by Pb, Sr and O isotope geochemistry (Weis and Demaiffe, 1983).

(3) Comparison between  $I_{Sr}$  values obtained for the various bodies and the contents in trace elements usually considered to be significant of crustal contamination (Rb, Ba, Th and K) does not show any correlation (Fig. 7). In particular, the Tellnes satellite dykes have the highest  $I_{Sr}$  value (0.710) and the lowest Rb and Ba contents. Moreover, preliminary Nd isotopic data (Demaiffe et al., 1986; Demaiffe and Weis, work in progress) indicate  $\epsilon_{Nd}(T)$  values varying from occurrence to occurrence between positive (+5.4 for the Tellnes ore) down to slightly negative (-1 for the Vettaland dyke). Samples with similar  $I_{Sr}$  values (0.7067 for the Håland dyke and 0.7069 for the Tellnes main dyke) have very different  $\epsilon_{Nd}$  values: -0.6 and +4.7 respectively. These data cannot be explained by a simple and single contamination process of a mantle-derived magma by crustal material. In a Nd-Sr isotopic diagram, the data for the different monzonorite occurrences do not define a trend, so that a single binary mixing model must be ruled out.

(4) On a smaller scale, large heterogeneities in the Sr isotopic composition can be maintained over small distances, as demonstrated in the apophysis by pillow-like inclusions which display distinctly lower  $I_{Sr}$  values than the mangerites with which they commingled. It is to be noted, moreover, that the mangerites, although appearing petrographically homogeneous, are quite variable isotopically.

### *Immiscibility*

Some rocks of the monzonoritic family should have appropriate compositions to enter the immiscibility field that, according to some authors (McBirney, 1975; Philpotts, 1981), separates SiO<sub>2</sub>-rich, granitic rocks from Fe-enriched liquids (ferrodiorites). Several arguments, however, indicate that this mechanism is not operating here, even in the case found in the apophysis, where field relationships (pillow-like inclusions) show good evidence of the existence of two liquids. Indeed, the latter differ considerably in their  $I_{Sr}$  values and thus cannot be derived from a common liquid. Moreover, the pillow-like inclusions show typical chilled textures, indicating that the two liquids were emplaced at different temperatures and thus could not be in equilibrium. Finally, there is no particular contrast in chemical composition between the two conjugated liquids (see Table I) as would be predicted, for example, for P<sub>2</sub>O<sub>5</sub>, REE, Zr and Ba on the basis of experimental data (Watson, 1976) and theoretical considerations (Ryerson and Hess, 1978).

### *Fractional crystallization*

The smooth trends displayed by the elements in variation diagrams can simply be explained by fractional crystallization. In bi-logarithmic diagrams, the analyses indeed plot on linear arrays, which points to a process controlled by the Rayleigh law. In the Tellnes main dyke, where the Sr isotopes assess the comagmatic character of the rocks and preclude contamination during fractionation, Wilmart et al. (1989) have calculated a quantitative model to account for the major and trace element evolution. Their method amplifies and improves a previous approach by Duchesne et al. (1985) on the Lomland dyke. It assumes a two-stage evolution and constrains the composition of the cumulate minerals which are subtracted from a liquid to move towards more evolved compositions by using the olivine-liquid Fe-Mg partition coef-

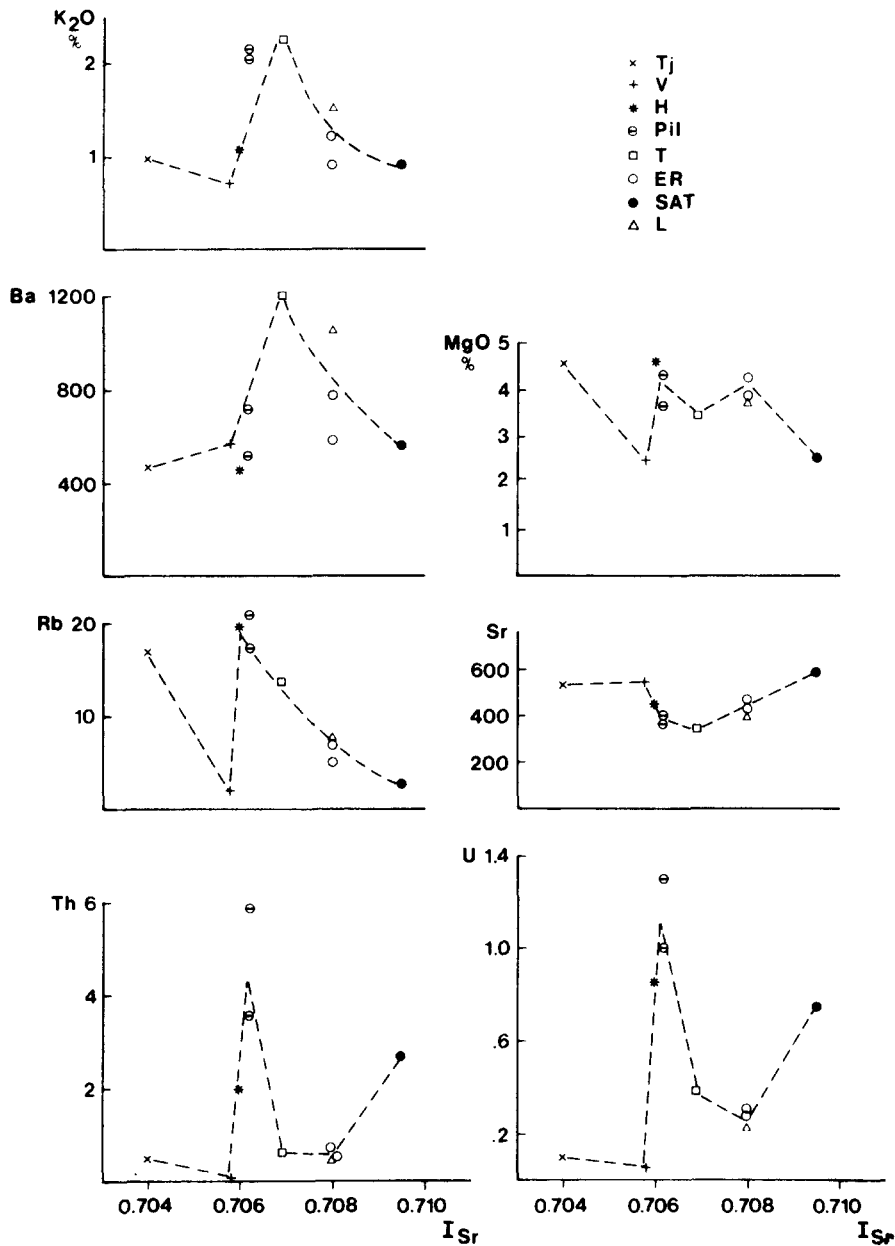


Fig. 7. Various element contents versus  $I_{Sr}$ . Trace elements in ppm. Tj, Tjörn chilled margin; V, Vettaland dyke; H, Hidra chilled margin; Pil, fine-grained monzonitic pillows in the apophysis; T, Tellnes dyke; ER, Eia-Rekefjord intrusion; SAT, Tellnes satellite dykes; L, Lomland dyke.

ficients of Ford et al. (1983). These permit the calculation of the Fe number of the olivine in equilibrium with a liquid of a given composition. The composition of the other cumulus minerals are then obtained by selecting the cumulate containing an olivine of this composi-

tion (or a corresponding orthopyroxene, when olivine is lacking) in the sequence of cumulates occurring in the neighbouring BKSK layered lopolith which has also crystallized from a monzonitic liquid in the same environment (Duchesne et al., 1987). Least-squares regres-

sion is finally used to calculate the proportion of the various cumulate minerals. A noritic cumulate made up of 42% plagioclase ( $An_{38}$ ) + 23% opx ( $En_{56}$ ) + 4% cpx ( $Wo_{44}En_{37}Fs_{19}$ ) + 9% ilmenite ( $Hem_4$ ) + 11% magnetite (5%  $TiO_2$ ) + 11% apatite subtracted from the less evolved monzonorite leads the liquid to a mangeritic composition. Subtraction from the mangerite of a second noritic cumulate with somewhat more evolved mineral compositions permits quartz mangerite to be reached.

The quantitative model also accounts for the trace element behaviour. Ba, Rb, Zr and Hf display an incompatible (or hygromagmaphile) behaviour, their contents increase with the inverse of the calculated fraction of residual melt. The REE content is mainly controlled by apatite fractionation. Values of apatite-liquid distribution around 10 are obtained, quite in agreement with those experimentally determined for similar magma composition and temperature (Watson and Green, 1981). The increase in the positive Eu anomaly in the successive liquids is explained by the simultaneous crystallization of plagioclase and apatite, the positive Eu anomaly of plagioclase being largely overbalanced by the negative anomaly of apatite (Roelandts and Duchesne, 1979). The relatively small variations of Nb-Ta and transition elements can also be explained by crystallization of Fe-Ti oxide minerals and pyroxenes.

The Tellnes model can also account for the evolution in the major and trace elements in the other occurrences (except the Vettaland dyke, which is discussed below). Thus subtraction of apatite-bearing noritic cumulates can explain the trends in the Håland and Lomland dykes as well in the Eia-Rekefjord intrusion (Fig. 2). Small differences in the composition of the cumulates, reflecting variations in the temperature and composition of the parental magmas, can be invoked to explain the characteristics of each occurrence. For instance, the decrease in the Zr-Hf content at the end of the Håland evo-

lution (Fig. 2b) implies that the Håland magma reached zircon saturation at about 62%  $SiO_2$ , which according to Watson and Harrison (1983) indicates a lower magma temperature than in Tellnes for the same  $SiO_2$  content.

The Tellnes model also precludes derivation of the various occurrences from a unique parental magma. The REE and the Hf-Zr contents of Hidra-Tjörn (HT), Sirevåg (S) and the Tellnes satellites (SAT) obviously cannot result from the fractional crystallization of the same magma.

The fractional crystallization process accounting for the geochemical evolution in the various units has not taken place inside the dykes or intrusions themselves, where no cumulate rocks are ever observed. It is therefore suggested that the series of liquids were produced, independently of each other, before the emplacement in relatively small magma chambers. A likely process of fractionation is sidewall crystallization and upward migration of the light residual liquid, as described by McBirney (1980).

The Vettaland dyke is an exception to the fractionation rule because the large variation in trace elements is only accompanied by a very small variation in major elements. Duchesne et al. (1985) have shown that partial melting in dry conditions of an apatite and plagioclase-bearing basic rock is a plausible formation process. Experiments by Baker and Egger (1987) on partial melting in dry conditions and at moderately high pressures (5–8 kbar) of high-alumina basalts remarkably confirm this deduction: ferromagmatic to monzonoritic liquids are obtained at low degrees of melting.

#### *Source of the monzonoritic magmas*

From the preceding discussion, it is concluded that the different magma batches that have given rise to the various monzonoritic units do not derive from a unique parental magma. The  $I_{Sr}$  and  $\epsilon_{Nd}(T)$  values indeed show a large interval of variation which cannot be explained

by a simple contamination process. The variation in some trace elements (Hf and REE contents) between the different units cannot be accounted for by the differentiation process: more probably, it reflects differences in the composition of each original magma batch.

The small positive Eu anomaly observed in most magma batches is difficult to explain if these are considered residual after the crystallization of massif-type anorthosites and if it is assumed, as commonly admitted (Emslie, 1978; Morse, 1982; Duchesne, 1984), that the parental magma of the anorthosites originated in the upper mantle. When considered together with the values of  $I_{Sr}$  (0.704–0.710) which are quite different from those of massif-type anorthosites (0.703–0.706), this character completely rules out the residual liquid hypothesis. The monzonorites are not comagmatic with massif-type anorthosites, and a direct derivation from the mantle is highly unlikely, at least for most of the occurrences.

Information on the mineralogy of the source rocks can be obtained by considering spidergrams (Fig. 4). If we discard K, Rb and Th, which might be partly metasomatically controlled in granulite facies conditions (see Glassey, 1983), troughs in Sr, Ti, Nb–Ta, and Hf–Zr are observed in most rocks. The depletion in these elements suggests that they have lost their incompatible behaviour in the melting process because, as major or minor elements, they entered into minerals remaining in the residue during the process. Sr can be present in plagioclase, Ti, Nb–Ta in Fe–Ti oxide minerals, and Zr–Hf in zircon. It is interesting to note that reconstruction of the source rock composition in the case of the Vettaland dyke (Duchesne et al., 1985) has also led to an apatite-bearing (ferro)noritic composition. It is therefore suggested that the source rocks of monzonoritic melts are basic to intermediate rocks of variable composition. In agreement with the  $I_{Sr}$  data, the Nd isotopic data confirm the distinct isotopic signature of each batch of monzonoritic magma. An origin by melting of variably

LREE depleted (positive  $\epsilon_{Nd}$ ) to undepleted ( $\epsilon_{Nd}$  close to zero) basic rocks is plausible in view of the isotopic data.

A new question arises from this conclusion: are apatite-bearing metabasites found in the lower crust? Two possible occurrences are suggested on the basis of the geological characteristics of southern Norway (Maijez and Padget, 1987). Basic to intermediate rocks of magmatic origin emplaced between 1.5 and 1.2 Ga (that is older than the anorthosite event) are found in the Bamble–Telemark area, such as the Morkeheia complex (Milne and Starmer, 1982). As an alternative, metabasites described in this area (Smalley and Field, 1985) or in Rogaland (Wilmart et al., 1987) are good candidates. Migmatization of metabasites can also play an important role in decoupling isotopes from the rest of the geochemical signature, but this hypothesis must be further worked out.

As for the heat necessary to trigger the partial melting process in the deep crust, it is closely related to the anorthosite magmatism. It can indeed be provided either by the hot anorthositic diapirs themselves on their way to final depth of emplacement (Duchesne et al., 1985), or by a regional enhancement of the heat flow responsible for the anorthosite magmatism.

## Conclusions

Monzonoritic rocks, though intimately related to massif-type anorthosites, are not residual after the formation of anorthosite. Notably variable in trace elements and isotopic composition, they show no evidence of contamination by crustal material. They probably result from the partial melting of (meta)basic rocks of variable composition in the deep crust.

Fractional crystallization with subtraction of apatite-bearing noritic cumulates can quantitatively account for their evolution towards K-rich rocks. This evolution can take place in a closed system, i.e., without contamination. In the anorthosite suite of rocks, monzonorite, mangerite and quartz mangerite, together with

cumulate norites and their derivatives, thus constitute a true series of rocks.

### Acknowledgements

E.W. wishes to thank M. Treuil and J.L. Joron for stimulating discussions and for providing full facilities for some NAA analysis. XRF analyses were performed at the Collectif Inter-universitaire de Géochimie Instrumentale, Liège University. The technical assistance of G. Bologne, G. Delhaze and V. Miocque is appreciated. The work was partly supported by the Fund for Basic Joint Research (Belgium). E.W. has benefited from a grant from the European Community.

### Appendix

#### *Analytical procedures*

X-Ray fluorescence on a CGR Lambda 2020 spectrometer (University of Liège) was used to analyze Si, Ti, Al, total Fe, Mn, Mg, Ca, K, P on Li borate glass discs, as well as Na, Rb, Sr, Zr, Y, Ni, Co, Zn, V, Cr, Ba, Ce, La and Nd, on pressed powder pellets. FeO was measured by titration.

Neutron activation analyses for REE, U, Th, Ta, Hf, Sc, Rb and Cr were carried out in three different laboratories: the Pierre Süe Laboratory, CEN, Saclay for the Håland, Tellnes and satellites dykes (Wilmart, 1988); the Afdeling Fysico-Chemische Geologie, KUL, Leuven, for the Hidra, Tjörn and Apophysis occurrences; the Mineralogisk-Geologisk Museum, Oslo University for the rest of the samples (Duchesne et al., 1985). The agreement between the different methods and the various laboratories is excellent. When several methods were used, the values from the NAA have been preferred. Rb and Sr concentrations were determined by X-ray fluorescence spectrometry except for some samples (see Table II) for which Rb was measured by isotope dilution. Sr was separated by conventional cation exchange techniques.

The Sr isotopic composition was measured by thermo-ionisation on a Finnigan MAT 260 mass spectrometer of the Belgian Centre of Geochronology. The  $^{87}\text{Sr}/^{86}\text{Sr}$  ratio of the NBS 987 standard is  $0.71022 \pm 0.00002$  ( $2\sigma$ ), normalized to  $^{88}\text{Sr}/^{86}\text{Sr} = 8.3752$ .

### References

- Ashwal, L.D., 1982. Mineralogy of mafic and Fe-Ti oxide-rich differentiates of the Marcy anorthosite massif, Adirondacks, New York. *Am. Mineral.*, 67: 14-27.
- Baker, D.R. and Eggler, D.H., 1987. Compositions of anhydrous and hydrous melts coexisting with plagioclase, augite, and olivine or low-Ca pyroxene from 1 atm to 8 kbar: application to the Aleutian volcanic center of Atka. *Am. Mineral.*, 72: 12-28.
- Buddington, A.F., 1972. Differentiation trends and parental magmas for anorthositic and quartz mangerite series, Adirondacks, New York. *Geol. Soc. Am. Mem.*, 132: 477-488.
- Demaiffe, D. and Hertogen, J., 1981. Rare earth geochemistry and strontium isotopic composition of a massif-type anorthositic-charnockitic body: the Hidra massif (Rogaland, S.W. Norway). *Geochim. Cosmochim. Acta*, 45: 1545-1561.
- Demaiffe, D., Weis, D., Michot, J. and Duchesne, J.C., 1986. Isotopic constraints on the genesis of the Rogaland anorthositic suite (Southwest Norway). *Chem. Geol.*, 57: 167-179.
- Duchesne, J.C., 1984. Massif anorthosites: another partisan review. In: W.S. Brown (Editor), *Feldspars and Feldspathoids*. NATO Advanced Study Institute, Series C137, pp. 411-433.
- Duchesne, J.C. and Demaiffe, D., 1978. Trace elements and anorthosite genesis. *Earth Planet. Sci. Lett.*, 38: 249-272.
- Duchesne, J.C., Denoiseux, B. and Hertogen, J., 1987. The norite-mangerite relationships in the Bjerkreim-Sokndal layered lopolith (SW Norway). *Lithos*, 20: 1-17.
- Duchesne, J.C. and Hertogen, J., 1988. Le magma parental du lopolithe de Bjerkreim-Sokndal (Norvège méridionale). *C.R. Acad. Sci. Ser. II*, 306: 45-48.
- Duchesne, J.C., Roelandts, I., Demaiffe, D., Hertogen, J., Gijbels, R. and De Winter, J., 1974. Rare-earth data on monzonoritic rocks related to anorthosites and their bearing on the nature of the parental magma of the anorthositic suite. *Earth Planet. Sci. Lett.*, 24: 325-335.
- Duchesne, J.C., Roelandts, I., Demaiffe, D. and Weis, D., 1985. Petrogenesis of monzonoritic dykes in the Egersund-Ogna anorthosite (Rogaland, S.W. Norway): trace elements and isotopic (Sr, Pb) constraints. *Contrib. Mineral. Petrol.*, 90: 214-225.
- Emslie, R.F., 1978. Anorthosite massifs, Rapakivi granites,

- and Late Proterozoic rifting of North America Precambrian Res., 7: 61–98.
- Emslie, R.F., 1985. Proterozoic anorthosite massifs. In: A.C. Tobi and J.L.R. Touret (Editors), *The Deep Proterozoic Crust in the North Atlantic Provinces*. NATO Advanced Study Institute, Series C158, pp. 39–60.
- Ford, C.E., Russel, D.G., Craven, J.A. and Fisk, M.R., 1983. Olivine-liquid equilibria: temperature, pressure and composition dependence on the crystal/liquid cation partition coefficients for Mg, Fe<sup>2+</sup>, Ca and Mn. *J. Petrol.*, 24: 256–265.
- Glassley, W.E., 1983. The role of CO<sub>2</sub> in the chemical modification of deep continental crust. *Geochim. Cosmochim. Acta*, 47: 597–616.
- Maijer, C. and Padget, P. (Editors), 1987. *The Geology of Southernmost Norway*. Norges Geol. Unders. Spec. Publ., 1: 109 pp.
- McBirney, A.R., 1975. Differentiation of the Skaergaard intrusion. *Nature (London)*, 253: 691–694.
- McBirney, A.R., 1980. Mixing and unmixing of magmas. *J. Volcan. Geotherm. Res.*, 7: 357–371.
- Michot, P., 1960. La géologie de la catazone : le problème des anorthosites, la paléogénèse basique et la tectonique catazonale dans le Rogaland méridional (Norvège méridionale). *Norg. Geol. Unders.*, 212g: 1–54.
- Michot, P., 1965. Le magma plagioclasiq. *Geol. Rundsch.*, 54: 956–976.
- Milne, K.P. and Starmer, I.C., 1982. Extreme differentiation in the Proterozoic Gjerstad–Morkeheia complex of South Norway. *Contrib. Mineral. Petrol.*, 79: 381–393.
- Morse, S.A., 1982. A partisan review of Proterozoic anorthosites. *Am. Mineral.*, 67: 1087–1100.
- Pasteels, P., Demaiffe, D. and Michot, J., 1979. U–Pb and Rb–Sr geochronology of the eastern part of the South Rogaland igneous complex, Southern Norway. *Lithos*, 12: 199–208.
- Philpotts, A.R., 1966. Origin of the anorthosite–mangerite rocks in Southern Quebec. *J. Petrol.*, 7: 1–64.
- Philpotts, A.R., 1981. A model for the generation of massif-type anorthosites. *Can. Mineral.*, 19: 233–253.
- Roelandts, I. and Duchesne, J.C., 1979. Rare-earth elements in apatite from layered norites and iron–titanium oxide orebodies related to anorthosites (Rogaland, S.W. Norway). In: L.H. Ahrens (Editor), *Origin and distribution of the elements*. Pergamon Press, Oxford, pp. 199–212.
- Ryerson, F.J. and Hess, P.C., 1978. Implications of liquid-liquid distribution coefficients to mineral-liquid partitioning. *Geochim. Cosmochim. Acta*, 42: 921–932.
- Smalley, P.C. and Field, D., 1985. Geochemical constraints on the evolution of the Proterozoic continental crust in Southern Norway (Telemark Sector). In: A.C. Tobi and J.L.R. Touret (Editors), *The Deep Proterozoic Crust in the North Atlantic Provinces*, NATO Advanced Study Institute, Series C158, pp. 551–566.
- Thompson, R.N., Morrison, M.A., Dickin, A.P. and Hendry, G.L., 1983. Continental flood basalts... Arachnids rule OK? In: C.J. Hawkesworth and M.J. Norry (Editors), *Continental Basalts and Mantle Xenoliths*. Shiva Publishing, Nantwich, pp. 158–185.
- Watson, E.B., 1976. Two-liquid partition coefficients: experimental data and geochemical implications. *Contrib. Mineral. Petrol.*, 56: 119–134.
- Watson, E.B. and Green, T.H., 1981. Apatite/liquid partition coefficients for the rare earth elements and strontium. *Earth Planet. Sci. Lett.*, 56: 405–421.
- Watson, B. and Harrison, M., 1983. Zircon saturation revisited: temperature and composition effects in a variety of crustal magma types. *Earth Planet. Sci. Lett.*, 64: 295–304.
- Weis, D. and Demaiffe, D., 1983. Pb isotope geochemistry of a massif-type anorthositic–charnockitic body: the Hydra massif (Rogaland, S.W. Norway). *Geochim. Cosmochim. Acta*, 47: 1405–1413.
- Wiebe, R.A., 1984. Commingling of magmas in the Bjerkreim–Sogndal lopolith (southwest Norway): evidence for the compositions of residual liquids. *Lithos*, 17: 171–188.
- Wilmart, E., 1988. Etude géochimique des charnockites du Rogaland. Doctorat thesis, Université Pierre et Marie Curie, Paris, 342 pp.
- Wilmart, E. and Duchesne, J.C., 1987. Geothermobarometry of igneous and metamorphic rocks around the Åna–Sira anorthosite massif: implications for the depth of emplacement of the South Norwegian anorthosites. *Nor. Geol. Tidsskr.*, 67: 185–196.
- Wilmart, E., Hertogen, J., Roelandts, I. and Duchesne, J.C., 1987. Geochemistry of Proterozoic supracrustals, granite–gneisses and charnockites from the envelope of the Åna–Sira anorthosite massif (Southwest Norway) (abstract). *Coll. IGCP 217 on Proterozoic Geochemistry*, Lund, 3–6 June.
- Wilmart, E., Demaiffe, D. and Duchesne, J.C., 1989. Geochemical constraints on the genesis of the Tellnes ilmenite deposit (S.W. Norway). *Econ. Geol.*, 84, in press.